Moisture buffer capacity of a bilayer bio- and geo-based wall

Méryl Lagouin, Aurélie Laborel-Préneron, Camille Magniont, Sandrine Geoffroy, Jean-Emmanuel Aubert

Moisture buffer capacity of a bilayer bio- and geo-based wall

Méryl LAGOUIN[1], Aurélie LABOREL-PRÉNERON[1], Camille MAGNIONT[1], Sandrine GEOFFROY[1], Jean-Emmanuel AUBERT[1]

[1] LMDC, Université de Toulouse, INSA, UPS, France

HIGHLIGHTS.

- sunflower-based concrete is highly hygroscopic and has self-insulating properties;
- glycerol carbonate limits shrinkage of earth plasters;
- clay-rich earth plaster exhibits higher sorption and moisture buffer capacity;
- a coupled heat and moisture transfer model satisfactorily estimates MBV.

ABSTRACT. The hygrothermal behaviour of bio- and geo-based bilayer wall assemblies is investigated. The highly hygroscopic nature and thermal insulating properties of a sunflower-based concrete make it a promising building material. However, vegetal concretes are usually coated to satisfy aesthetic requirements. Therefore, the finishing layer is taken into consideration when investigating the hygrothermal behaviour of a wall. To improve the heat and mass storage and transport properties, without jeopardizing the general behaviour of plasters, an organically admixed mortar formulation was developed and the hygrothermal properties of each layer (sunflower concrete and plaster) were determined experimentally. The data were included in a coupled heat and moisture transfer 1D-model, which was applied to simulate the hygrothermal behaviour of the sunflower concrete specimen coated with earth plaster. The comparison of numerical moisture buffer values with experimental data for the wall assembly gave satisfactory results in spite of the heterogeneity of the materials and the experimental uncertainty. As expected, the numerical results show that the bilayer structure with the optimised plaster exhibits higher moisture buffer capacities than one with the reference formulation.

KEYWORDS. bio-based concrete, earthen plaster, bilayer wall, hygrothermal properties, moisture buffer value, simulation.

1. Introduction

The use of environmentally friendly materials with good thermal and hygroscopic properties appears to be a good way of reducing the environmental impact of buildings. Among such materials, bio-based concretes exhibit satisfactory thermal properties and, more importantly, high hygric abilities. Their thermal conductivity is approximately 0.1 W/(m.K) [1], so these composites can be considered as self-insulating materials. Moreover, the use of such material buffers indoor humidity, delays the transmission of outside climate variations and improves indoor air quality more efficiently than other traditional walls: its water vapour resistance factor usually ranges from 5 to 12 [2]–[10] and its Moisture Buffer Value (MBV) is higher than 2 g/(m².%RH) [7]–[9], [11]–[14]. Hence, vegetal concretes help to reduce energy needs while maintaining good indoor comfort.

Nevertheless, in practice, bio-based concrete walls are coated for aesthetic reasons and the use of coating or inner layers can influence the moisture buffering ability of the vegetal concrete wall.

Since they are less porous than vegetal concretes, plasters present higher thermal conductivity and vapour resistance factor, and weaker hygroscopic behaviour [15]. Consequently, the coating induces an additive vapour resistance that reduces and delays the vapour transfer through the wall [16], [17]. However, it does not stop the sorption-desorption and/or the evaporation-condensation phenomena in vegetal concrete, preserving their breathing properties as underlined by Collet and Prétot [16], [18] and Aït Ouméziane *et al.* [19].

As the storage and transfer potentials are altered by the presence of a plaster, the moisture buffering capacity of the multi-layer structure is likely to decrease. Colinart *et al.* [15], Maalouf *et al.* [20] and Tran Le *et al.* [21] have shown that the use of a less hygroscopic material on the surface of a vegetal concrete wall lowers the vapour exchange between the wall and the atmosphere inside the room. The ability of the wall to attenuate ambient variations in relative humidity is thus reduced by 15 to 50%; the humidity amplitude is greater in the presence of a plaster [15], [20]–[22]. However, Latif *et al.* [12] pointed out that adding 18 mm of lime plaster did not significantly reduce the MBV of lime-hemp concrete. The coating did not compromise the water capacity of the bio-based wall, which remained excellent. The numerical simulations by Evrard and De Herde [23] on hemp concrete characterised by Evrard [3] seem to agree with this observation. These opposite observations show the dependence of the materials' properties on ambient variation attenuation abilities of the wall assembly. When the substrate and the coating exhibit similar storage and transfer potentials, the moisture buffering capacity of the multi-layer structure is less impacted.

The thickness of coating plays a key role in the capacity of the wall to capture, transfer and store moisture [17], [19]. For a given coating formulation, numerical simulations show that the increase in thickness lowers the quantity of moisture in the vegetal concrete: the relative humidity in hemp concrete, at a depth of 8 cm, decreased by 45 to 47% when the plaster thickness increased from 3 to 5 cm [19].

Regarding mix design, sand-lime or hemp-lime coatings are usually applied to bio-based walls. Their higher porosity gives lime-based plasters stronger sorption capacities than conventional ones [17], [24]. The ability to mitigate hygric variations is more marked inside the wall when the pores are interconnected and the water vapour permeability of the plaster is high. Among the coatings applied and characterised, earth-based plasters showed the best performances in terms of moisture buffer capacity, comfort, and energy consumption [22], [25]. The clay-based formulations appear to be promising and should therefore be favoured for the coating of walls made of vegetal concrete.

The limited environmental impact [26] and the positive effect of earth plasters on hygric comfort [13], [27], [28] have already been proved. As hygric regulators, clayish plasters are considered as good, or even excellent, their MBV ranging from 1.1 to 3.7 g/(m².%RH) [13], [27], [28]. The moisture buffering effect of unfired clay plaster has demonstrated the strong influence of clay content and the mineralogy involved on indoor humidity. The works of McGregor *et al.* [28] and Palumbo *et al.* [29] consider that the nature of the soil (grain size and mineralogy) has a major effect on the MBV. Kaolinite-based materials exhibited a limited buffering ability compared to coatings formulated with clays having stronger sorption properties [29].

The work reported in the present paper aimed to develop a high-performance hygrothermal bilayer wall composed of a sunflower-based concrete coated with an earth plaster. The choice of the two constitutive materials of the wall for this study was based on previous works [30], [31], in which the formulations have demonstrated their high potential as self-insulating/self-supporting wall filling material and interior plaster, respectively. Their performance as components of a bilayer structure is discussed here.

The two layers are characterised individually in the first part of this article, regarding their water sorption and vapour permeability behaviours as well as thermal conductivity and specific heat capacities. The second part of the study is dedicated to the assessment of the assembly with both experimental and numerical approaches for the estimation of the buffering potential of such a bilayer structure.

2. Materials and methods

2.1. Sunflower-based concrete

Previous work led to the definition of the design and manufacturing procedure for the vegetal concrete produced here [30]. This material is composed of sunflower bark aggregates and a metakaolin-based pozzolanic binder.

New specimens of Metakaolin-Sunflower concrete were produced, according to the same mix proportions and methodology as the one defined in [30]. Vegetal concrete specimens were manufactured in cylindrical moulds 11 cm in diameter and 6 cm in length for water vapour permeability tests, and cast in 15 cm x 15 cm x 15 cm moulds for moisture buffering tests.

2.2. Unfired clay plasters

The earth plasters studied were composed of earth, a siliceous river sand (0-2 mm) and tap water. The soil selected for this study was investigated in previous work [31], [32]. It was composed of quarry fines from aggregate washing processes.

Various proportions of sand and water were mixed with the earth to design a valid plaster regarding shrinkage cracks. The plaster with the highest earth to sand ratio that did not exhibit cracks was selected as the reference formulation. The selected formulation was designed with 15% earth content (i.e. soil to sand ratio of 1:6.5).

The combination of two admixtures, Flax Fibre (FF) and Glycerol Carbonate (GC), was tested here to develop a high-clay-content earth plaster. Previous work to evaluate the potential of organic stabilisers [31] had demonstrated that, among six admixtures, only flax fibre showed sufficient crack reduction to meet the aesthetic and mechanical requirements for indoor plastering. This study also explores the effects of glycerol carbonate addition. This additive was prepared from a renewable raw material, glycerol, which is generated by the chemical conversion of vegetable oils. Glycerol is thus a co-product in the industrial productions of fatty acids (surface active agents) and of biodiesel [33]. Glycerol carbonate was used by Magniont *et al.* [33] as a green admixture in a hydraulic lime and metakaolin-based binder. This work demonstrated the positive effect of glycerol carbonate on the reduction of shrinkage: thanks to its low surface tensions in the capillary fluid, the level of microcracking was significantly reduced.

In all cases, mortars were prepared by using the mixing procedure:

- mix the clay and sand at low speed;
- add water to the solid phase and adjust the amount to ensure a flow table value of 175 ± 5 mm as proposed in the German standard [34], while mixing at low speed;
- mix the mortar at higher speed;
- stop the mixer and leave the mixture to rest for a few minutes;
- complete mixing at high speed.

When required, glycerol carbonate was mixed with water before being incorporated into the solid phase. In contrast, fibres were added directly into the wet mixture. The water content of fresh plaster was measured by drying at 60°C.

2.1. Manufacturing of coated samples

The plasters were applied either on a fibrewood panel or on a sunflower-based concrete. Either way, the substrate was oiled and sprayed with water in advance. Once dry, the substrate was lightly and evenly water sprayed again immediately before the application of a plaster coating. The fresh mortar was the directly applied to the prepared substrate with light impulsion. The plaster was easily levelled using a wooden frame and a trowel. The thickness of the plasters was either 1 cm or 2 cm.

2.2. Procedures

2.2.1. Shrinkage assessment

The shrinkage test was conducted according to the procedure proposed in [35]: an earth plaster is considered to be of acceptable mechanical quality if, after shrinkage, there are no cracks through which water can penetrate into the wall and if the plaster is not detached (even partially) from the substrate.

After drying, the presence or absence of cracks in two 25 x 25 cm² and 1 cm thick plaster samples per formulation was detected by image analysis. The cracking assessment was processed by numerical isolation of the fissures using Matlab and a specific algorithm. This work enabled the cumulative developed length of cracks to be characterised quantitatively.

Regarding the coating adherence, shear tests are performed: samples were loaded by a 2 kg device, which corresponded to the plaster self load with a safety coefficient of 10, considering a thickness of 30 mm. If, after 30 seconds, all specimens resisted the load, it was considered that the substrate had been well prepared and that the mortar was of sufficient quality [36]. The assembly was identical to the one presented in [31].

2.2.2. Mercury porosimetry

Tests were performed using an AutoPore IV 9500 (Micromeritics) mercury porosimeter, which has a measuring range of 0.0007-420 MPa. Common values of γ and α were used [37]–[39]: the mercury surface tension was 485 J/m² and the contact angle was 140°.The contact angle, α, was assumed to be constant during intrusion and extrusion. Total porosity and pore size distribution were obtained over the entire operating diameter range (from 0.4 nm to 400 µm). Before testing, samples were dried in an oven at 50°C.

Two samples of each material were tested to check that the mercury intrusion behaviour was similar for both.

2.2.3. Hygric properties

Sorption isotherms

Dynamic Vapour Sorption (DVS) is a gravimetric technique that measures the amount of water that is adsorbed by a sample at equilibrium. First, the test specimens were dried in the DVS for 3 hours at 60°C. The sorption isotherm was measured at 23°C, according to the standard EN NF ISO 12571 [40]. The amount of water adsorbed was measured at successive stages of increasing relative humidity: 0, 20, 40, 60, 80 and 95% RH. The water content was calculated from the dry mass of the specimen. For each step, moisture balance was considered to be reached in the specimen when the mass variation [%] over the period of time (dm/dt) was less than 5.10^{-5}%/min over a ten-minute period or in a maximum time interval of 720 min for the first three steps, 1440 min for 60 and 80% RH and 2160 min for the last step.

Water vapour permeability

Tests were performed on three cylindrical specimens 6 cm in height and 11 cm in diameter. Both the wet and dry cup methods were applied as specified in standard NF EN ISO 12572 [41]. Before testing, samples were stored and were initially in equilibrium with air at 25 ± 1°C and 60 ± 5% RH. The criterion for equilibrium was that the weight of the sample must have stabilized so that two successive daily determinations (24 hours apart) of the weight agreed to within 0.1% of the mass of the test specimen.

The specimen was positioned in an aluminium cup in such a way as to avoid contact with the saline solution, which was placed at the bottom of the cup (**Figure 1**). The whole set- up was surrounded by an aluminium tape at the junction of the support and the specimen. The system was placed in a climatic chamber regulated at 25 ± 1°C and 60 ± 5% RH and ventilated so that the air velocity at the surface of each specimen was greater than 2 m/s. The relative humidity in the cup was controlled by a saturated salt solution of potassium nitrate (93.58 ± 0.55% at 25°C) for the wet cup and of sodium hydroxide

(8.24 ± 2.1% at 25°C) for the dry cup, while the relative humidity around the cup was controlled by air conditioning. The gradient of relative humidity created an outgoing flow of water vapour in the case of the wet cup and an incoming flow with the dry cup.

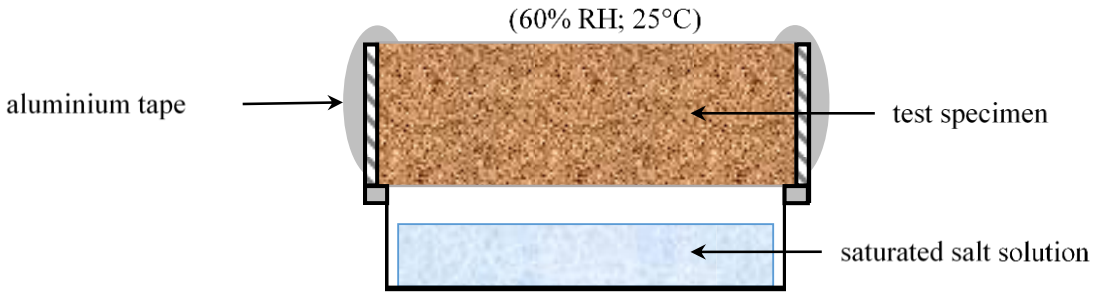

Figure 1. Test cup scheme adapted from Vololonirina and Perrin **[42]**.

The systems were weighed regularly until a steady-state vapour flux was reached. The transmission rate of water vapour through the sample, G, determined by linear regression of the kinetics of mass and the water vapour permeability, δ_P, was then deduced:

$$G = \frac{\Delta m}{\Delta t} \quad (1)$$

$$\delta_P = \frac{e}{\frac{A.\Delta P_v}{G} - \frac{d_a}{\delta_{P,a}}} \quad (2)$$

where G is the mass flow rate [kg/s],
Δm, mass variation [kg],
t, time [s],
$\delta_{P,a}$, water vapour permeability [kg/(m.s.Pa)],
d, thickness of the specimen [m],
d_a, thickness of the air gap [m]
A, exposed surface area [m²],
ΔP_v, vapour pressure difference [Pa].

The vapour pressure was calculated using:

$$P_v = (RH_2 - RH_1) * 610.5 * e^{\frac{17.269T}{237.3+T}} \quad (3)$$

where RH_1 and RH_2 are the relative humidity inside and outside the cup, respectively [%], T is the temperature [K] and $\delta_{P,a}$ is the water vapour permeability in air [kg/(m.s.Pa)]. The air permeability can be expressed by the Schirmer formula. At 25°C and standard atmospheric pressure, $\delta_{P,a}$ = 1.96 10^{-10} kg/(m.s.Pa).

The water vapour diffusion resistance factor, μ, corresponds to the ratio of the diffusion coefficients of water vapour in air and in the building material. Thus, it represents the factor by which the vapour diffusion in the material is impeded with respect to diffusion in stagnant air. For very permeable materials, such as mineral wool, the resistance factor is close to 1 whereas impermeable materials show a much higher value. For instance, polyethylene sheet resistance factor ranges from 50 000 to 320 000.

Moisture buffer value

The moisture buffering performances of the specimens were assessed according to the NORDTEST protocol [43]. For each the wall assembly, measurements were conducted on four specimens of bio-aggregate-based materials (7.5 x 7.5 x 15 cm^3) coated with 1 cm or 2 cm of earth-based plaster. Before testing, the test specimens were sealed on all but the coated side with aluminium tape. Then they were stored and initially in equilibrium with the air at 23 ± 5°C and 50 ± 5% RH. The test specimens were placed in a climatic chamber where the air velocity was about 0.1 ± 0.05 m/s, set to expose samples to a daily relative humidity cycle (8 hours at 75% RH - 16 hours at 33% RH). The temperature was kept constant at 23°C.

The weight gains and losses of samples were tracked with an accuracy of 0.01 g using an adaptation of the NORDTEST protocol: instead of the frequently recommended technique, the samples were weighed twice per cycle, immediately before the change of RH step, to minimize the disturbances caused by frequent opening of the climatic chamber.

The NORDTEST protocol determined the MBV value at the steady state, i.e. when, for three consecutive cycles, the material satisfied the following conditions: change in mass, Δm [g], less than 5% between the last three cycles; and difference between weight gain and weight loss within each cycle less than 5% of Δm. In each cycle, Δm was determined as the average of the weight gain during the moisture uptake branch of the cycle and the weight loss during drying. The steady state was reached after about 3 weeks of daily variation.

2.2.4. Thermal properties

Thermal conductivity

The thermal conductivity of the dried materials was measured by the hot wire transient method. This technique consists of placing a shock probe between two pieces of material so that power can be broadcast and the rise of temperature within the material can be measured.

This transient method only allows local measurements. To tackle the question of accuracy and representativeness for heterogeneous materials such as plant concrete, thermal conductivity was defined as the average of at least ten measurements. For each formulation, the device was placed at several locations on different samples. Due to the anisotropic arrangement of vegetal concretes in the sunflower-based concrete, the hot wire was located in a plane parallel to the direction of compaction of the specimens, in diverse positions. The measured value therefore corresponds to an intermediate value between conductivity in the directions parallel and perpendicular to the direction of compaction. Nevertheless, deviation from the mean value was only of 7%. A Neotim-FP2C hot wire apparatus was used for this study. The heat flow and heating time were chosen so that a temperature rise higher than 5°C and a correlation coefficient between experimental data and theoretical behaviour higher than 0.999 could be reached.

Specific heat capacity

The specific heat capacity of a material is its ability to store thermal energy. The method used was based on detecting the changes of temperature and heat flow caused by endothermic and exothermic processes of the materials. A direct measurement was made by means of differential scanning calorimetry (DSC) on each component of earth plaster and sunflower based concrete.

DSC measurements followed standard ISO 11357-4 [44], using a continuous-scan programme in which the temperature increased from about 16°C to 140°C. The heating rate was 20 K/min. One measurement was performed for each material. The specific heat capacity was then determined at 23°C.

To overcome problems of the representativeness of small samples taken from composite materials, determination of the heat capacity of the composite materials in the dry state was based on the specific heat capacities of each component:

$$c_p^{dry} = \sum_i x_i \, c_{p,i} \tag{4}$$

From the dry specific heat capacity, the heat capacity at 50% RH could be estimated:

$$c_p = \frac{1}{1+u} c_p^{dry} + \frac{u}{1+u} c_{p,water} \tag{5}$$

with u the moisture content [kg/kg] and $c_{p,water}$ the specific heat capacity of water ($c_{p,water}$ = 4187 J/(kg.K)). This method of calculation was previously used and validated by Seng *et al.* [45].

3. Numerical simulation

The experimentally measured properties of the two materials were used as input data for the numerical simulations of the moisture buffering behaviour of the coated bio-based concrete. The model was implemented in the FEM software COMSOL, using the Partial Differential Equations module.

3.1. Heat and mass transfer

The model developed by Seng *et al.* [46] was used for the heat and moisture transfer in 1D through the earth plaster and sunflower concrete layers in the wall. The resulting system of equations describing the moisture transfer, energy transfer and moisture phase change rate are the following:

$$\begin{cases} \dfrac{\partial w}{\partial P_C}\dfrac{\partial P_C}{\partial t} = -\boldsymbol{\nabla}\left[\left(\delta_{P,l} + \delta_{P,v}\dfrac{\rho_v}{\rho_l}\right)\boldsymbol{\nabla} P_C - \delta_{P,v}\left(RH\dfrac{\partial P_v^{sat}}{\partial T} - p_v\dfrac{ln(RH)}{T}\right)\boldsymbol{\nabla} T\right] \\ \left(\rho_s c_{p,s} + \sum_i w_i \, c_{p,i}\right)\dfrac{\partial T}{\partial t} = \lambda \, \boldsymbol{\nabla}^2 T - \left[(c_{p,l} - c_{p,v})T - L_v\right]S_l - \sum_i w_i \, \boldsymbol{\mathcal{V}}_i c_{p,i}\boldsymbol{\nabla} T \\ \left(\dfrac{1}{1 - \rho_v/\rho_l}\right)\dfrac{\partial w}{\partial t} = -\boldsymbol{\nabla}\left(\delta_{P,l}\boldsymbol{\nabla}\boldsymbol{P_C}\right) + S \end{cases} \tag{6}$$

where w is the total moisture content [kg/m^3] and w_i the moisture content [kg/m^3] with $i = l$ for liquid water and $i = v$ for water vapour,

$\delta_{P,l}$ and $\delta_{P,v}$ are respectively the liquid and vapour permeabilities [kg/(m.s.Pa)],

ρ_l, ρ_v and ρ_s are respectively the liquid water, the water vapour and the material apparent densities [kg/m^3],

P_v is the vapour pressure [Pa] and P_v^{sat} is the saturated vapour pressure [Pa],

$c_{p,i}$ is the specific heat capacity of water vapour or liquid water [J/(kg.K)],

λ is the material thermal conductivity [W/(m.K)],

$\boldsymbol{\mathcal{V}}_i$ is the velocity of water vapour or liquid water [m/s] and L_v is the latent heat of vaporisation [J/kg].

The parameters studied were the capillary pressure P_C [Pa], the temperature T [K] and the source term S, which corresponds to the moisture phase change rate [kg of moisture/m^3 of material/s].

3.2. Initial values and boundary conditions

The boundary conditions between the outer wall layer and the air in the climatic chamber were described with a convective heat flux q_{conv} [W/m²] and a convective mass transfer flux g_m [kg/(m².s)].

$$\begin{cases} q_{conv} = h_{conv}\,(T_{air,surf} - T_{air}) \\ g_m = h_m\,(P_{v,surf} - P_{v,air}) \end{cases} \quad (7)$$

where h_{conv} is the convective heat transfer coefficient (= 2.5 W/(m².K) based on NF EN 15026 [47]) and h_m is the convective mass transfer coefficient [kg/(m².s.Pa)]. Based on scale analysis, the latent effect was found negligible and thus is not considered in the boundary condition of the thermal equation [46].

Temperature and capillary pressure continuity were considered at the interface between material and air cavity:

$$\begin{cases} T_{air,surf} = T_{mat,surf} \\ P_{c,air} = P_{c,surf} \end{cases} \quad (8)$$

As a multi-layered building material, the coated sunflower concrete wall requires us to focus on the interface when choosing the contact. Even though there may be some air pockets at the interface between the two composites, the contact is assumed to be perfect. In consequence, heat and moisture flows are continuous between layers, which implies that vapour and capillary pressures are continuous across the interface.

4. Results and discussion

4.1. Sunflower-based concrete hygrothermal characterisation

4.1.1. Hygric properties

Vegetal concrete adsorption isotherms were determined in a previous work [30]. From this measurement, it was possible to determine the moisture capacity in the 33-75%RH range: this value is of 0.057 kg/kg, which demonstrates the great hygroscopicity of the material.

Complementary tests were carried out to characterise the hygric behaviour of the sunflower-based concrete. Water vapour permeability tests were conducted according to both the wet and the dry cup methods. Average values are given in **Table 1**.

	Water vapour permeability, δ [x10^{-11} kg/(m.s.Pa)]	**Water vapour diffusion resistance factor, μ [-]**
Dry cup (8-60% RH)	15.0 ± 5.2	1.4 ± 0.4
Wet cup (60-93% RH)	13.9 ± 4.4	1.5 ± 0.5

Table 1. Average water vapour permeability and resistance factor of sunflower concrete.

While surprisingly close, the water vapour permeability values obtained with the two assembly types attest to the high permeability of the tested material to water vapours. This result is consistent with the very open porous structure (71.5 ± 5.3% of open pores) revealed by both mercury intrusion porosimetry and X-ray tomography in [30].

The diffusion resistance values are in accordance with the results obtained previously [30], for the same material mix design used for a different batch. The values were found to be much lower than factors from the literature [3], [5], [7]–[9], ranging from 4 to 12. This difference can be attributed to test parameters as stated by Vololonirina and Perrin [42], in particular to the relative humidities applied. Tests were conducted under 10/60%RH and 60/93%RH conditions here, while most authors determine water vapour permeability under 0/50%RH and/or 50/93%RH. Due to surface diffusion and capillary condensation, which become noticeable at higher humidities, the variation of local relative humidity

from the values found in literature is likely to explain the higher values of water vapour permeability encountered in the present study. As evidenced by Chamoin *et al.* [6], for hygroscopic materials, the water vapour permeability increases with relative humidity.

Moreover, the air velocity on the surface of the specimens also seems to impact significantly the water vapor flow. Even if the minimum value of 2 m/s as recommended for highly porous materials in the standard NF EN ISO 12572 [41] is verified, it can be observed that air velocity varying between 2 and 4 m/s leads to water vapor permeability values quite distinct. The influence of this parameter was not properly assessed in this study and to the authors' knowledge, no publication on the matter is yet available.

4.1.2. Thermal performances

The thermal conductivity value of concrete was determined in [30]. It is recalled, along with the measured and calculated heat capacities of the sunflower and metakaolin-based concrete, in **Table 2**.

		Bio-based concrete	
		Metakolin-based binder paste	**Sunflower aggregate**
Mass ratio [%]		0.69	0.31
Specific heat capacity at 23°C [J/(kg.K)]		870	1541
Heat capacity [J/(kg.K))	**dry state**	1078	
	50% RH	1184	
Density [kg/m³]		461.71 ± 16.27	
Thermal conductivity [W/(m.K)]		0.128 ± 0.009 [46]	

Table 2. Thermal properties of the vegetal concrete.

The specific heat capacity of the self-insulating material is consistent with results from other studies. In the literature, the specific heat capacity of bio-based concretes varies between 770 and 1560 J/(kg.K) [2], [3], [37], [48], [49].

4.2. Clay-rich plaster

4.2.1. Optimal plaster formulation research

The objective of this work phase was to define an earth-based coating formulation that was richer in clay minerals than a reference formulation (5% of clay minerals) and not stabilized, without compromising its mechanical behaviour. Thanks to the effect of additives, a higher clay content in plaster should improve the hygric performance of earthen materials.

To check that the mechanical performances of the plaster were not compromised, two tests were carried out: the shrinkage cracking of dry plasters was evaluated before the adhesion between the plaster and its substrate was tested. This methodology, developed by Hamard *et al.* [35], aims to assess the validity of a coating formulation and its compatibility with the substrate. A plaster is valid from a mechanical standpoint when, after drying, it shows no cracks through which water could penetrate and is not detached, even partially, from the support.

In order to guarantee the maximum objectivity of the comparative analysis of mortar cracking, a Matlab program was developed. Two elements were considered to quantify the cracking network: the cumulative length of cracks on a plaster specimen and the percentage of cracked surface compared to the total surface area of the wall coated were evaluated. Thus, for each formulation tested, quantified data were obtained, cumulating crack lengths or surface areas for the two 250 x 250 mm² plaster specimens.

Table 3 summarizes the formulations tested to maximise the clay content in plaster while guaranteeing the absence of shrinkage defects.

	Earth content [%]	Admixture	Cracking
Reference formulation	15	-	no
Cracking reduction test formulations	20	-	first non-stabilised formulation exhibiting cracks
	20	0.5% flax fibres	no
	20	1% glycerol carbonate	no
	33	-	yes
	33	0.75% flax fibres + 2% glycerol carbonate	few small cracks
Optimised	33	0.75% flax fibres + 1% glycerol carbonate	no

Table 3. Summary of the tested formulations.

The effect of the adjuvants on the cracking of the plasters was first assessed in relation to the mortar having a 20% soil content (**Figure 2**), which was the first non-stabilised formulation exhibiting cracks potentially compromising the durability of the wall. **Figure 3** shows the evolution of cracking on the surface of the plaster specimens thanks to the addition of 0.5% by mass of the solid phase in the form of flax fibres or 1% of glycerol carbonate.

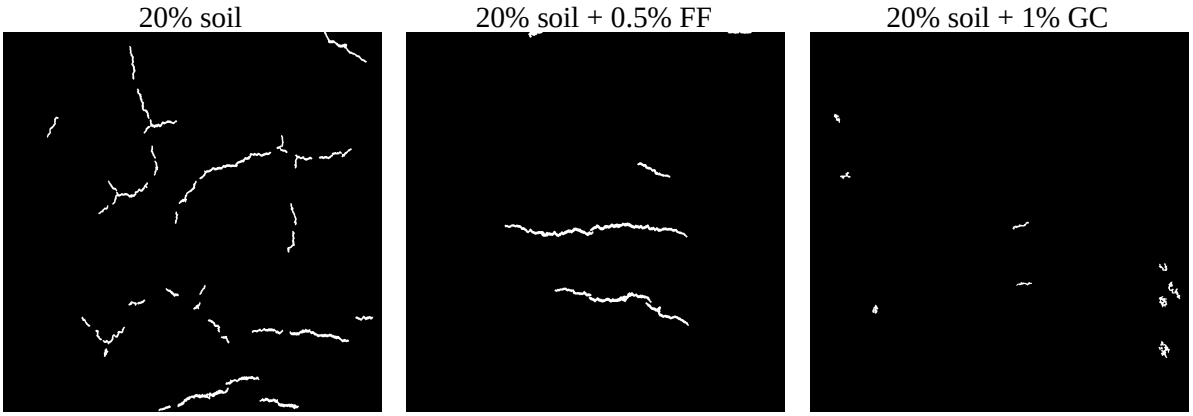

Figure 2. Shrinkage test binarised images.

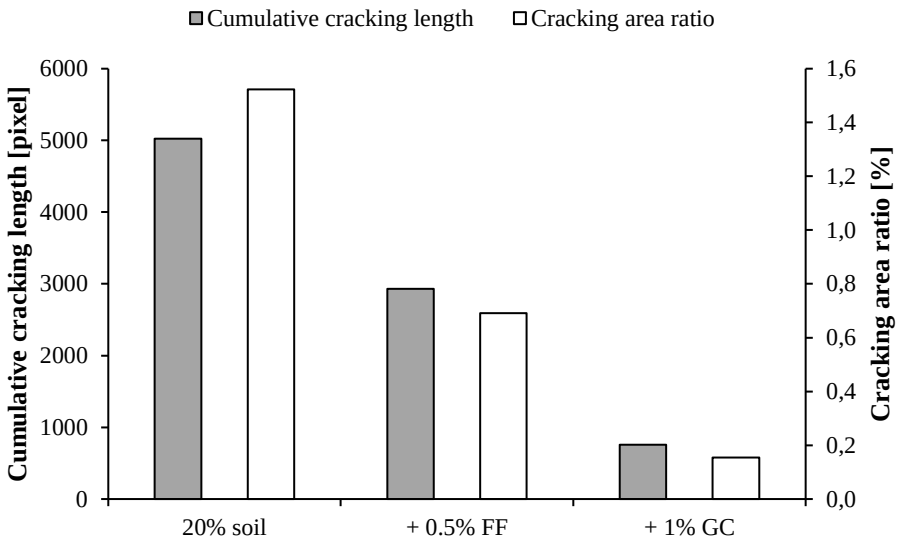

Figure 3. Evaluation of the reinforcement effect of flax fibres (FF) and glycerol carbonate (GC) through cumulative cracking length and cracking area ratio assessment.

These measurements highlight the efficacy of the two adjuvants tested in reducing the cracking of 20% soil plasters. The cumulative length of the cracks is halved as a result of flax fibre reinforcement, while the glycerol carbonate allows a reduction by a factor of 10 compared to the non-adjuvanted formulation. These additives therefore have a high potential for decreasing the cracking of earth plasters.

For the formulations richest in clay, a search for the optimal amount of adjuvant was undertaken. For 33% soil plaster, the fibre content had to be increased - but without exceeding 0.75% in order to meet workability requirements. The effect of glycerol carbonate, introduced at 1% or 2%, was also investigated. **Figure 4** shows the impact of glycerol carbonate content on the 33% soil mix reinforced with 0.75% flax fibres.

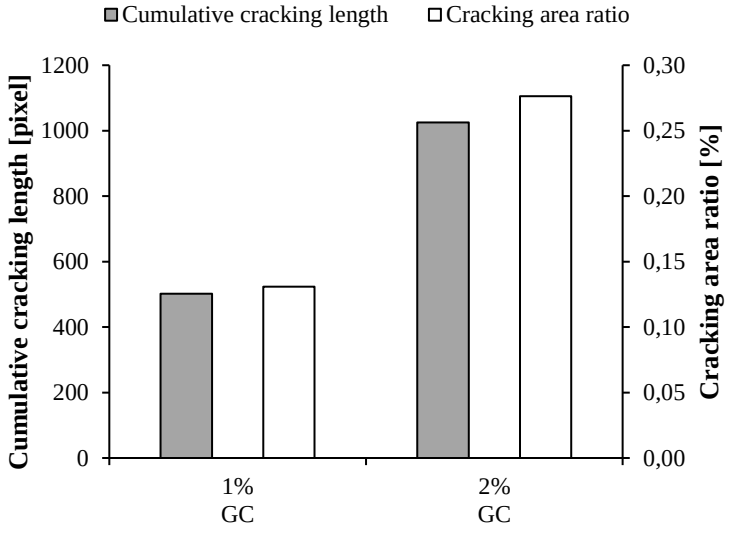

Figure 4. Evaluation of the impact of glycerol carbonate on the cracking reduction of 33% soil + 0.75% FF formulation.

It has emerged from this numerical assessment that increasing the surfactant content does not necessarily have a beneficial effect on reducing cracking. While the addition of 1% glycerol carbonate greatly helps the reduction of shrinkage cracks, doubling the dose is likely to have a deleterious effect.

This observation was also expressed by Magniont *et al.* [50] regarding pozzolanic-based binder paste. The incorporation of up to 1% glycerol carbonate induces an increase in the amount of water evaporated

from the capillary pores, generating limited shrinkage as the evaporation of the capillary water leads to only little capillary tension, due to the larger diameter of the capillary pores [51]. Magniont *et al.* demonstrated the existence of a limit concentration of glycerol carbonate, beyond which the total shrinkage of the admixed paste rose again. The dose was about 1.5% for pozzolanic binder. This outcome is consistent with the trends found in present study.

In view of the cracking analyses carried out, the formulation containing 33% of earth, admixed with 1% of glycerol carbonate and reinforced with 0.75% of flax fibres was selected as the optimal formulation.

To ensure its validity, a shear stress test was conducted. The compatibility with the substrate (i.e. the sunflower-based concrete characterised in Section 4.14.1) was tested for both the non-admixed 15% earth-based plaster and the optimised formulation plaster. Since no specimen collapsed under loading, the plasters are considered as satisfactory with regard to their mechanical behaviour. Their hygrothermal performances can therefore be evaluated.

4.2.2. Physical and hygrothermal characterisation

Porous structure and apparent density

The porous structure was evaluated by means of mercury porosimetry measurements. The results, along with apparent density values, are given in **Table 4**.

	Apparent density [kg/m^3]		**Total porosity [%]**
	measured by MIP	**geometrical measurement**	
15% earth-based plaster	1917 ± 22	1881 ± 39	31.2 ± 0.4
33% earth-based admixed plaster	1593 ± 46	1601 ± 38	41.2 ± 0.8

Table 4. Physical properties of earth-based plasters studied.

The density of the materials is in the 1500 - 2000 kg/m^3 range, and thus in accordance with the results available in literature on clayish coatings [27], [29], [52]–[60]. The effect of clay content on density differences was not obvious. While Lima *et al.* [58] witnessed a slight upward trend in bulk density when the clay fraction was greater, Gomes *et al.* [56] noted the opposite effect.

On the other hand, the addition of vegetal particles tends to lower the density of earthen plasters [27], [56], [60]–[62], as agroresources, occupying a volume no longer filled with clay matrix, have a lower density than the latter, so the plaster density is logically lowered.

Moreover, the porosity exploration within plasters epitomized the evolution of the volume of voids between the non-stabilised formulation and the optimised one. In the range of pores explored, the total porosities of the coatings were found to be 31.19 ± 0.35% for the raw mix and 41.19 ± 0.77%, for the optimised formulation. These total porosity values are in agreement with studies by other authors, which generally report open porosities ranging from 25 to 40% [27], [55], [56], [59], [60], [63], [64].

In particular, the present results show that the optimised formulation clearly has a greater quantity of void than the non-stabilised mortar does, with a variation of 32%. To better understand the origin of this change in the porous structure, the pore distributions of the two plasters are presented in **Figure 5.**

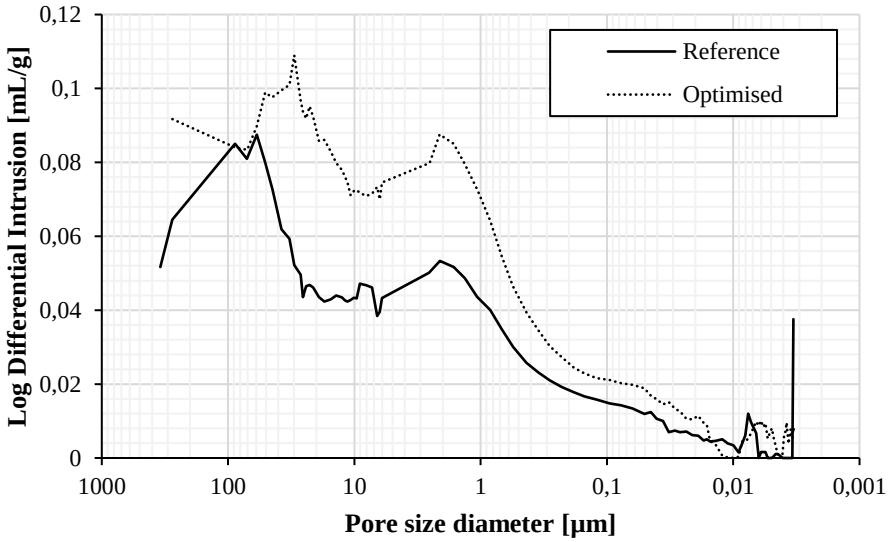

Figure 5. Pore size distributions, with and without optimisation of earth-based plasters.

In both cases, two main pore families can be identified: a peak between 1 and 6 µm and a second one corresponding to pores larger than 20 µm are evidenced. It can be noted that the pore distribution of the plaster without admixture is largely preserved despite the organic additions. Regarding the pore families, only the peak related to cavities with a diameter ranging from 30 to 300 µm on the 15% soil-based plaster is shifted; their size is reduced, passing into the 10-70 µm range when stabilised.

The figure shows a clear increase in the amount of voids irrespective of the size. More specifically, the greater presence of pores with diameters larger than 100 µm can be pointed out. This finding is consistent with the values obtained regarding the total porosity of materials.

Thanks to their large porous network, earth plasters have the ability to capture, store and transport both water and heat.

Sorption isotherms

The sorption capacities of plasters are plotted in **Figure 6**.

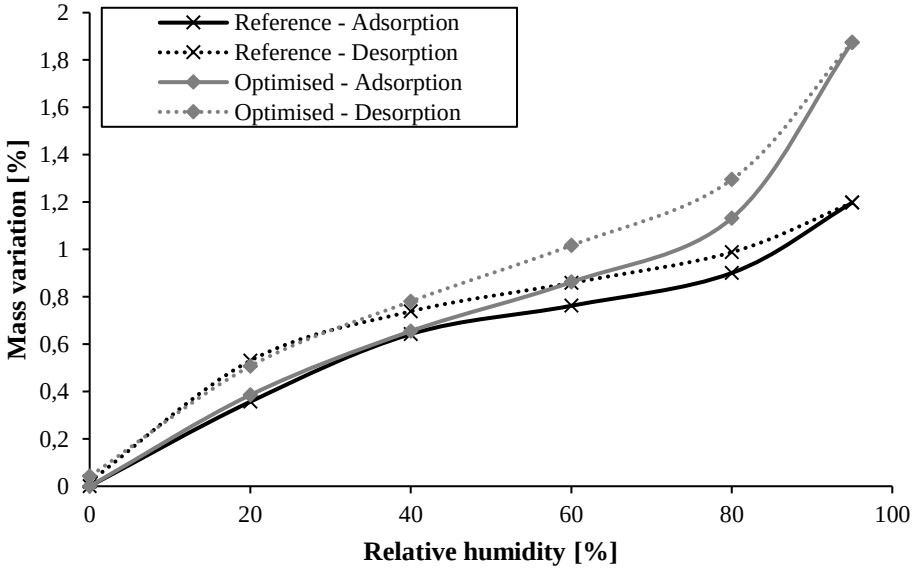

Figure 6. Sorption isotherms of basic plaster without admixture and optimised coating formulation.

The sorption curves show the same sigmoidal shape, type II according to the IUPAC classification [65], characteristic of macro- and mesoporous media. At low and medium humidities, the two formulations tested achieve similar sorption capacities with, at 40% RH, a moisture content of approximately 0.7% in the adsorption phase and 0.8% in desorption. It can come from the fact that, for smaller pores, the two coatings show similar pore size distribution which is consistent with a comparable sorption capacity below 40% RH in the monolayer adsorption domain. Beyond 40% RH, the optimised material has higher moisture storage capacity than the plaster without admixture, reaching nearly 2% at saturation state, compared with 1.2% in the case of the sandy mix design. In the range of 33-75%RH, the moisture capacity of the optimised formulation (0.0124 kg/kg) is about twice as high as the reference one (0.0066 kg/kg). The differences are marked on high relative humidity levels in the area of capillary condensation in large pores since the optimised coating exhibits a larger volume of pores than the reference plaster.

This behaviour is in agreement with the adsorption capacities of earthen plaster described by McGregor *et al.* [28] and confirmed by the greater void content in optimised plasters as evidenced by the mercury porosimetry measurements. The difference between the moisture-trapping properties of the two tested clayish materials is consistent with the increased clay content between the benchmark formulation and the optimised mortar, the amount of clay in the latter being twice as high as in the former. The sorption capacities of earthen materials are known to be mainly dictated by clay minerals: the decrease in clay content in plasters, due to sand additions, leads to a significant decrease in the hygroscopic properties of the material [58]. The presence of vegetal particles would also tend to promote moisture absorption according to some authors [27], [64], [66], [67].

Water vapour permeability

The permeability measurements were carried out according to both the wet and the dry cup methods. The values of permeability and water vapour diffusion resistance factors are given in **Table 5**.

	Water vapour permeability [x 10^{-11} kg/(m.s.Pa)]		**μ [-]**	
Formulation	**dry cup**	**wet cup**	**dry cup**	**wet cup**
Reference	4.0 ± 1.0	6.3 ± 2.1	5.2 ± 1.3	3.3 ± 1.1
Optimised	3.4 ± 0.1	5.9 ± 2.2	5.8 ± 0.2	3.4 ± 0.6

Table 5. Test results of the water vapour permeability and diffusion resistance factor obtained by dry and wet cup methods.

The difference in water vapour permeability values between the two formulations are within the measurement margin of error. It is therefore not possible to formally conclude on the evolution of the moisture transfer capacities of the optimised plaster formulation compared to non-admixed mortar. These mixed results might be explained by the fact that the previously evidenced increase in porosity, thanks to adjuvantation, can be counterbalanced by the effects of the plant particle additions. Such additions are likely to reduce the connectivity of the capillary pores, thus lowering their ability to transport moisture, as observed by Laborel-Préneron [68].

The water vapour resistance factor is about 3 for the wet cup test, while it ranges from 5.9 to 6.3 when the dry cup test is used. As mentioned in Evrard *et al.* [3], the vapour permeability measured with the wet cup method is usually higher than dry cup results. In the opinion of the authors, referring to Krus [1996], the difference between moist and dry values is due to a liquid flow superimposed on vapour diffusion.

Moreover, the values obtained in this study are below values found in the literature for earthen plasters, where the factors generally vary between 4 and 15 for the wet cup test. This difference may also be justified by the moisture transportation modes involved, among other things. In the same way as for bio-based concrete, this parameter is directly dependent on the choice of the hygrometries applied on either side of the material. The increase in vapour permeability with the ambient humidity leads to surface liquid diffusion, in a first phase, followed by a capillary condensation for the moistest conditions [6]. In the literature, the relative humidity on the outer side of the material under test is usually 50% RH

(0-50% RH for the dry cup and 50-93%RH for the wet cup). Here, the outside humidity was set at 60% RH and the inside value was 8%RH. It can therefore be supposed that the liquid transport occurring along with vapour diffusion is greater at 60% RH than at 50% RH, leading to higher water vapour permeability values.

Finally, a strong dispersion of the measurements can also be noted. It can be explained by the heterogeneity of air velocity inside the climatic chamber, which can differ from one specimen to another.

Thermal conductivity

Table 6 shows the thermal conductivity of earth plasters.

Formulation	Density [kg/m^3]	Thermal conductivity [W/(m.K)]
Reference	1881 ± 39	0.629 ± 0.051
Optimised	1601 ± 38	0.518 ± 0.036

Table 6. Density and thermal conductivity of earth plasters in dry conditions.

With a thermal conductivity of approximately 0.5-0.7 W/(m.K), the earth plasters studied cannot be considered as thermal insulators. The values obtained are consistent with scientific literature data regarding earth plasters [27], [29], [55]–[58], [60]–[62]. Insulating properties have been found to be highly dependent on the density, even though density alone does not allow the thermal conductivity of earthen plasters to be defined.

The thermal conductivities of the two coatings can therefore be largely explained by their composition. Although sandy materials have better insulating properties than highly clayish plasters [56], [62], due to the presence of plant fibres, the reference formulation exhibits higher thermal conductivity than the optimised mix design, richer in clay particles. This result is mainly explained by the increase in porosity and, thus, the decrease in mortar density.

Specific heat capacity

Based on the mass ratios and specific heat capacities of the mortar constituents, the heat capacity of earth plasters can be determined. **Table 7** summarises the 50% RH heat capacity calculations.

Composite	Raw material	Mass ratio [%]	Specific heat capacity at 23°C [J/(kg.K)]	Heat capacity [J/(kg.K)]	
				Dry state	50% RH
Reference	sand	0.15	679	979	1001
	earth	0.85	1032		
Optimised	sand	0.66	679	742	766
	earth with 1% GC	0.33	843		
	flax fibres	0.01	1789		

Table 7. Heat capacity and emissivity determination based on specific heat capacity measurements.

The heat capacity values obtained for earth plasters are higher for the reference formulation than for the optimised one. This finding underlines their greater ability to store thermal energy. These values are consistent with results from the literature, which vary between 640 and 1000 J/(kg.K) for earthen materials [40], [77]–[82].

The results emphasize the significant influence of the porous structure on the hygrothermal behaviour of the plaster. While the standard deviation of the water vapour permeability does not allow to draw any conclusion on the impact of the tested formulation, higher moisture storage ability is evidenced for more porous materials, especially for relative humidities higher than 40%. The higher void content in the optimised plaster is responsible for the lower density and thus for the greater insulating potential.

However, the more porous and hence lighter materials, the lower their capacity to store heat and to delay its transmission.

4.3. Moisture buffering capacity of the coated wall

4.3.1. Comparison between simulation and experimentation

The Moisture Buffer Value calculated according to the Nordtest protocol is given in **Figure 7**.

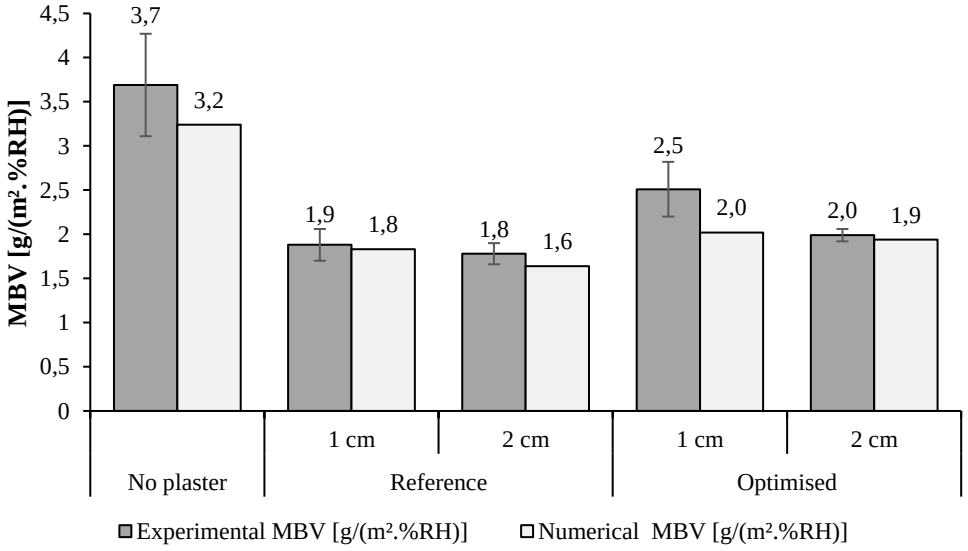

Figure 7. Numerical estimations and experimental results of the moisture buffer value of bilayer walls.

Both methods agree on the fact that the tested wall assemblies can be considered as good – or, in some cases, even excellent – hygric buffering materials.

Numerical moisture buffer values for the wall assemblies give results that are quite satisfactory compared to experimental findings since boundary conditions were not strictly identical and, given the heterogeneity of the materials (composition, air velocity and thickness) and the experimental uncertainty, theoretical values differ from the experimental results to a certain extent, particularly for the 1 cm optimised wall assembly. Except for the last-mentioned formulation, the deviation between the simulation and experimentation data is within the experimental margin of error.

4.3.2. Influence of plastering

A value of 3.7 ± 0.6 g/(m².% RH) was measured experimentally for uncoated sunflower concrete. When the concrete substrate was coated with an earth-based plaster, the MBV was reduced by 32 to 52%, to a value ranging from 1.7 to 2.5 g/(m².% RH), depending on the thickness and formulation of the coating. A similar trend was observed with numerical values: the MBV was reduced by 30 to 40%. This confirms that the coating with less hygroscopic and permeable materials reduces the moisture buffer value of building materials. When comparing hemp concrete coated with lime-based plasters to uncoated concrete, Lelièvre *et al.* [75] observed a 40% deviation. Despite these moisture buffering capacity decreases, the performances recorded for the sunflower and earth-based wall assemblies still fall within the good, or even excellent, class of the moisture buffering materials classification.

From a plaster formulation standpoint, both experimental results and numerical simulations are likely to present a higher MBV of the assemblies with optimised plaster than the ones with the reference mortar formulation, as intended. The higher clay content and the fibre additions contribute an MBV increase of about 10 and 30% for the 1 cm and 2 cm coated walls, respectively, compared to the reference coated assembly wall. It can also be pointed out that the plaster thickness influences more the specimens coated

with optimised plaster than with the reference one. This is reminiscent of the theoretical concept of penetration depth: the additive vapour resistance that reduces and delays the vapour transfer through the wall is plausibly greater for the reference plaster and consequently, the penetration depth is lower than for the optimised formulation. Consequently, increasing the thickness of the plaster is of greater influence on the penetration depth of the more porous plaster. Similar results can be found in [22].

Finally, both experimental and numerical outcomes underline the impact of plaster thickness on the MBV of the wall assemblies. As the coating is less hygroscopic than the sunflower substrate, the moisture buffering capacity is lowered when the plaster thickness increases from 1 to 2 cm, regardless of the coating formulation. Thus, the experimental MBVs are reduced by 5 to 20%, for the reference and optimised plasters respectively. The impact of plaster thickness has already been reported in the literature [17], [19], [22].

5. Conclusion

The present paper focused on investigating the hygrothermal behaviour of bio- and geo-based bilayer wall assemblies. The sunflower formulated concrete developed in a previous work was characterised for a wall filling application. Its highly hygroscopic and thermal insulating properties make this plant-based concrete a promising building material.

However, bio-based materials are usually coated to satisfy aesthetic requirements within a building. Therefore, the finishing layer must be considered when investigating the hygrothermal behaviour of building materials. In earth-based plasters, the clayey phase gives the global cohesion of the plaster and is responsible for the dry strength, the water vapour permeability and the sorption capacity of earthen plasters. However, clay also induces drying shrinkage of the mortar, leading to cracking of the plaster. One of the objectives of this work was to improve the moisture buffer capacity of earthen plaster by increasing its clay content without jeopardizing the general behaviour of plasters. Based on numerical cracking control and a shear test, an optimised formulation was developed. Organic admixture and plant fibre addition allowed the clay content to be more than doubled. The optimised material was assessed on its hygrothermal properties, comparing its performances with a non-stabilized, low-clay-content earth plaster.

Finally, a coupled heat and moisture transfer 1D-model was applied to simulate the hygrothermal behaviour of the coated sunflower concrete specimen with earth-based plaster. The experimentally determined hygrothermal properties of each layer (sunflower concrete and plasters) were included in the model. Perfect contact was assumed between the two layers. The comparison of numerical moisture buffer values with experimental data for the wall assembly gave satisfactory results in spite of the materials' heterogeneity and the experimental uncertainty. As expected, the numerical results showed that the bilayer structure with the optimised plaster had higher moisture buffer capacities than the one with the reference formulation. The use of such a model could be an alternative to experimental measurements of the MBV to estimate the moisture buffering capacity of bilayer walls with variable coating layer compositions more quickly. Further investigations could be carried out to increase the model accuracy, taking hysteresis and temperature/humidity dependencies into consideration for all input data.

6. References

[1] H. H. Ratsimbazafy, A. Laborel-Préneron, C. Magniont, et P. Evon, « A Review of the Multi-Physical Characteristics of Plant Aggregates and Their Effects on the Properties of Plant-Based Concrete », p. 69, juin 2021.

[2] F. Collet *et al.*, « Caractérisation hydrique et thermique de matériaux de Génie Civil à faibles impacts environnementaux », Institut National des Sciences Appliquées de Rennes, Rennes, 2004.

[3] A. Evrard, « Transient hygrothermal behaviour of Lime-Hemp Materials », p. 142, 2008.

[4] B. Haba, B. Agoudjil, A. Boudenne, et K. Benzarti, « Hygric properties and thermal conductivity of a new insulation material for building based on date palm concrete », *Construction and Building Materials*, vol. 154, p. 963-971, nov. 2017, doi: 10.1016/j.conbuildmat.2017.08.025.
[5] R. Walker et S. Pavía, « Moisture transfer and thermal properties of hemp–lime concretes », *Construction and Building Materials*, vol. 64, n° Supplement C, p. 270-276, août 2014, doi: 10.1016/j.conbuildmat.2014.04.081.
[6] J. Chamoin, « Optimisation des propriétés (physiques, mécaniques et hydriques) de bétons de chanvre par la maîtrise de la formulation », INSA de Rennes, 2013.
[7] F. Collet, J. Chamoin, S. Pretot, et C. Lanos, « Comparison of the hygric behaviour of three hemp concretes », *Energy and Buildings*, vol. 62, p. 294-303, juill. 2013, doi: 10.1016/j.enbuild.2013.03.010.
[8] M. Rahim *et al.*, « Characterization of flax lime and hemp lime concretes: Hygric properties and moisture buffer capacity », *Energy and Buildings*, vol. 88, p. 91-99, févr. 2015, doi: 10.1016/j.enbuild.2014.11.043.
[9] M. Rahim, O. Douzane, A. D. Tran Le, G. Promis, et T. Langlet, « Characterization and comparison of hygric properties of rape straw concrete and hemp concrete », *Construction and Building Materials*, vol. 102, p. 679-687, janv. 2016, doi: 10.1016/j.conbuildmat.2015.11.021.
[10] A. D. Tran Le, « Etude des transferts hygrothermiques dans le béton de chanvre et leur application au bâtiment (sous titre: simulation numérique et approche expérimentale) », Université de Reims Champagne-Ardenne, Reims, 2010. [En ligne]. Disponible sur: tel-00590819v4
[11] F. Collet et S. Pretot, « Experimental investigation of moisture buffering capacity of sprayed hemp concrete », *Construction and Building Materials*, vol. 36, p. 58-65, nov. 2012, doi: 10.1016/j.conbuildmat.2012.04.139.
[12] E. Latif, M. Lawrence, A. Shea, et P. Walker, « Moisture buffer potential of experimental wall assemblies incorporating formulated hemp-lime », *Building and Environment*, vol. 93, p. 199-209, nov. 2015, doi: 10.1016/j.buildenv.2015.07.011.
[13] M. Palumbo, A. M. Lacasta, N. Holcroft, A. Shea, et P. Walker, « Determination of hygrothermal parameters of experimental and commercial bio-based insulation materials », *Construction and Building Materials*, vol. 124, p. 269-275, oct. 2016, doi: 10.1016/j.conbuildmat.2016.07.106.
[14] R. V. Ratiarisoa, C. Magniont, S. Ginestet, C. Oms, et G. Escadeillas, « Assessment of distilled lavender stalks as bioaggregate for building materials: Hygrothermal properties, mechanical performance and chemical interactions with mineral pozzolanic binder », *Construction and Building Materials*, vol. 124, n° Supplement C, p. 801-815, oct. 2016, doi: 10.1016/j.conbuildmat.2016.08.011.
[15] T. Colinart, D. Lelievre, et P. Glouannec, « Experimental and numerical analysis of the transient hygrothermal behavior of multilayered hemp concrete wall », *Energy and Buildings*, vol. 112, p. 1-11, janv. 2016, doi: 10.1016/j.enbuild.2015.11.027.
[16] F. Collet et S. Pretot, « Experimental highlight of hygrothermal phenomena in hemp concrete wall », *Building and Environment*, vol. 82, p. 459-466, déc. 2014, doi: 10.1016/j.buildenv.2014.09.018.
[17] M. Bart, S. Moissette, Y. Ait Oumeziane, et C. Lanos, « Transient hygrothermal modelling of coated hemp-concrete walls », *European Journal of Environmental and Civil Engineering*, vol. 18, n° 8, p. 927-944, sept. 2014, doi: 10.1080/19648189.2014.911122.
[18] F. Collet et S. Prétot, « Effect of coating on moisture buffering of hemp concrete », in *The Second International Conference on Building Energy and Environment*, Boulder, United States, août 2012, p. 878-885. Consulté le: 25 janvier 2019. [En ligne]. Disponible sur: https://hal.archives-ouvertes.fr/hal-00767893
[19] Y. Aït Ouméziane, S. Moissette, M. Bart, et C. Lanos, « Effect of coating on the hygric performance of a hemp concrete wall », in *5th IBPC*, Kyoto, Japan, mai 2012, p. 109-116. Consulté le: 24 avril 2020. [En ligne]. Disponible sur: https://core.ac.uk/reader/48210579

[20] C. Maalouf, A. D. T. Le, S. B. Umurigirwa, M. Lachi, et O. Douzane, « Study of hygrothermal behaviour of a hemp concrete building envelope under summer conditions in France », *Energy and Buildings*, vol. 77, p. 48-57, juill. 2014, doi: 10.1016/j.enbuild.2014.03.040.
[21] A. D. Tran Le, C. Maalouf, T. H. Mai, E. Wurtz, et F. Collet, « Transient hygrothermal behaviour of a hemp concrete building envelope », *Energy and Buildings*, vol. 42, n° 10, p. 1797-1806, oct. 2010, doi: 10.1016/j.enbuild.2010.05.016.
[22] M. Labat, C. Magniont, N. Oudhof, et J.-E. Aubert, « From the experimental characterization of the hygrothermal properties of straw-clay mixtures to the numerical assessment of their buffering potential », *Building and Environment*, vol. 97, p. 69-81, févr. 2016, doi: 10.1016/j.buildenv.2015.12.004.
[23] A. Evrard et A. De Herde, « Hygrothermal Performance of Lime-Hemp Wall Assemblies », *Journal of Building Physics*, vol. 34, n° 1, p. 5-25, juill. 2010, doi: 10.1177/1744259109355730.
[24] Y. Aït Oumeziane, « Evaluation des performances hygrothermiques d'une paroi par simulation numérique: application aux parois en béton de chanvre », p. 354, 2013.
[25] S. Liuzzi, M. R. Hall, P. Stefanizzi, et S. P. Casey, « Hygrothermal behaviour and relative humidity buffering of unfired and hydrated lime-stabilised clay composites in a Mediterranean climate », *Building and Environment*, vol. 61, p. 82-92, mars 2013, doi: 10.1016/j.buildenv.2012.12.006.
[26] P. Melià, G. Ruggieri, S. Sabbadini, et G. Dotelli, « Environmental impacts of natural and conventional building materials: a case study on earth plasters », *Journal of Cleaner Production*, vol. 80, p. 179-186, oct. 2014, doi: 10.1016/j.jclepro.2014.05.073.
[27] S. Liuzzi *et al.*, « Hygrothermal properties of clayey plasters with olive fibers », *Construction and Building Materials*, vol. 158, p. 24-32, janv. 2018, doi: 10.1016/j.conbuildmat.2017.10.013.
[28] F. McGregor, A. Heath, A. Shea, et M. Lawrence, « The moisture buffering capacity of unfired clay masonry », *Building and Environment*, vol. 82, p. 599-607, déc. 2014, doi: 10.1016/j.buildenv.2014.09.027.
[29] M. Palumbo, F. McGregor, A. Heath, et P. Walker, « The influence of two crop by-products on the hygrothermal properties of earth plasters », *Building and Environment*, vol. 105, p. 245-252, août 2016, doi: 10.1016/j.buildenv.2016.06.004.
[30] M. Lagouin, C. Magniont, P. Sénéchal, P. Moonen, J.-E. Aubert, et A. Laborel-préneron, « Influence of types of binder and plant aggregates on hygrothermal and mechanical properties of vegetal concretes », *Construction and Building Materials*, vol. 222, p. 852-871, oct. 2019, doi: 10.1016/j.conbuildmat.2019.06.004.
[31] M. Lagouin, A. Laborel-Préneron, C. Magniont, S. Geoffroy, et J.-E. Aubert, « Effects of organic admixtures on the fresh and mechanical properties of earthbased plasters », *Journal of Building Engineering*, p. 24, 2020.
[32] M. Lagouin, J.-E. Aubert, A. Laborel-Préneron, et C. Magniont, « Influence of chemical, mineralogical and geotechnical characteristics of soil on earthen plaster properties », *Construction and Building Materials*, vol. 304, p. 124339, oct. 2021, doi: 10.1016/j.conbuildmat.2021.124339.
[33] C. Magniont, G. Escadeillas, C. Oms-Multon, et P. De Caro, « The benefits of incorporating glycerol carbonate into an innovative pozzolanic matrix », *Cement and Concrete Research*, vol. 40, n° 7, p. 1072-1080, juill. 2010, doi: 10.1016/j.cemconres.2010.03.009.
[34] DIN 18947, « Lehmputzmörtel e begriffe, anforderungen, prüfverfahren ». août 2013.
[35] E. Hamard, J.-C. Morel, F. Salgado, A. Marcom, et N. Meunier, « A procedure to assess the suitability of plaster to protect vernacular earthen architecture », *Journal of Cultural Heritage*, vol. 14, n° 2, p. 109-115, mars 2013, doi: 10.1016/j.culher.2012.04.005.
[36] FFB, RESEAU écobâtir, Fédération des SCOPBTP, et École Nationales des Travaux Publics de l'État, « Règles professionnelles pour la mise en oeuvre des enduits sur supports composés de terre crue », *Recherche et développement métier*, 2012.
[37] A. Bourdot *et al.*, « Characterization of a hemp-based agro-material: Influence of starch ratio and hemp shive size on physical, mechanical, and hygrothermal properties », *Energy and Buildings*, vol. 153, p. 501-512, oct. 2017, doi: 10.1016/j.enbuild.2017.08.022.

[38] F. Collet, M. Bart, L. Serres, et J. Miriel, « Porous structure and water vapour sorption of hemp-based materials », *Construction and Building Materials*, vol. 22, n° 6, p. 1271-1280, juin 2008, doi: 10.1016/j.conbuildmat.2007.01.018.
[39] Y. Jiang, M. Lawrence, M. P. Ansell, et A. Hussain, « Cell wall microstructure, pore size distribution and absolute density of hemp shiv », *Royal Society Open Science*, vol. 5, n° 4, p. 171945, avr. 2018, doi: 10.1098/rsos.171945.
[40] AFNOR, « Performance hygrothermique des matériaux et produits pour le bâtiment - Détermination des propriétés de sorption hygroscopique ». octobre 2000.
[41] AFNOR, « Performance hygrothermique des matériaux et produits pour le bâtiment - Détermination des propriétés de transmission de la vapeur d'eau - Méthode de la coupelle ». octobre 2016. Consulté le: 16 septembre 2020. [En ligne]. Disponible sur: https://viewer.afnor.org/Pdf/Viewer/?token=73KMzdInqI81
[42] O. Vololonirina et B. Perrin, « Inquiries into the measurement of vapour permeability of permeable materials », *Construction and Building Materials*, vol. 102, p. 338-348, janv. 2016, doi: 10.1016/j.conbuildmat.2015.10.126.
[43] C. Rode *et al.*, *Moisture buffering of building materials*, Department of Civil Engineering Technical University of Denmark. 2005.
[44] AFNOR, « Plastiques - Analyse calorimétrique différentielle (DSC) », 30 août 2014. https://viewer.afnor.org/Pdf/Viewer/?token=HjkiSN-4r141 (consulté le 24 août 2020).
[45] B. Seng, C. Magniont, et S. Lorente, « Characterization of a precast hemp concrete. Part I: Physical and thermal properties », *Journal of Building Engineering*, vol. 24, p. 100540, juill. 2019, doi: 10.1016/j.jobe.2018.07.016.
[46] B. Seng, S. Lorente, et C. Magniont, « Scale analysis of heat and moisture transfer through bio-based materials — Application to hemp concrete », *Energy and Buildings*, vol. 155, p. 546-558, nov. 2017, doi: 10.1016/j.enbuild.2017.09.026.
[47] AFNOR, « Performance hygrothermique des composants et parois de bâtiments - Évaluation du transfert d'humidité par simulation numérique ». avril 2008. Consulté le: 18 septembre 2020. [En ligne]. Disponible sur: https://viewer.afnor.org/Pdf/Viewer/?token=vFxyuHtjubw1
[48] E. Gourlay, P. Glé, S. Marceau, C. Foy, et S. Moscardelli, « Effect of water content on the acoustical and thermal properties of hemp concretes », *Construction and Building Materials*, vol. 139, p. 513-523, mai 2017, doi: 10.1016/j.conbuildmat.2016.11.018.
[49] B. Seng, « Etude expérimentale et numérique du comportement hygrothermique de blocs préfabriqués en béton de chanvre », Université de Toulouse, Université Toulouse III-Paul Sabatier, Toulouse, 2018.
[50] C. Magniont, « Contribution à la formulation et à la caractérisation d'un écomatériau de construction à base d'agroressources », Université de Toulouse, Université Toulouse III-Paul Sabatier, 2010.
[51] A. M. Neville, *Propriétés des bétons*, 1ère édition. Eyrolles, 2000. Consulté le: 7 septembre 2020. [En ligne]. Disponible sur: https://www.editions-eyrolles.com/Livre/9782212013207/proprietes-des-betons
[52] T. Ashour et W. Wu, « An experimental study on shrinkage of earth plaster with natural fibres for straw bale buildings », *International Journal of Sustainable Engineering*, vol. 3, n° 4, p. 299-304, déc. 2010, doi: 10.1080/19397038.2010.504379.
[53] R. Delinière, J. E. Aubert, F. Rojat, et M. Gasc-Barbier, « Physical, mineralogical and mechanical characterization of ready-mixed clay plaster », *Building and Environment*, vol. 80, p. 11-17, oct. 2014, doi: 10.1016/j.buildenv.2014.05.012.
[54] A. Fabbri, F. McGregor, I. Costa, et P. Faria, « Effect of temperature on the sorption curves of earthen materials », *Materials and Structures*, vol. 50, n° 6, déc. 2017, doi: 10.1617/s11527-017-1122-7.
[55] P. Faria, T. Santos, et J.-E. Aubert, « Experimental Characterization of an Earth Eco-Efficient Plastering Mortar », *J. Mater. Civ. Eng.*, vol. 28, n° 1, p. 04015085, janv. 2016, doi: 10.1061/(ASCE)MT.1943-5533.0001363.

[56] M. I. Gomes, P. Faria, et T. D. Gonçalves, « Earth-based mortars for repair and protection of rammed earth walls. Stabilization with mineral binders and fibers », *Journal of Cleaner Production*, vol. 172, p. 2401-2414, janv. 2018, doi: 10.1016/j.jclepro.2017.11.170.
[57] J. Lima, P. Faria, et A. S. Silva, « Earth-based plasters: the influence of clay mineralogy », in *5th Historic Mortars Conference HMC2019*, Pamplona, Spain, juill. 2019, p. 21-35.
[58] J. Lima, P. Faria, et A. Santos Silva, « Earthen Plasters Based on Illitic Soils from Barrocal Region of Algarve: Contributions for Building Performance and Sustainability », *KEM*, vol. 678, p. 64-77, févr. 2016, doi: 10.4028/www.scientific.net/KEM.678.64.
[59] T. Santos, P. Faria, et V. Silva, « Can an earth plaster be efficient when applied on different masonries? », *Journal of Building Engineering*, vol. 23, p. 314-323, mai 2019, doi: 10.1016/j.jobe.2019.02.011.
[60] T. Santos, L. Nunes, et P. Faria, « Production of eco-efficient earth-based plasters: Influence of composition on physical performance and bio-susceptibility », *Journal of Cleaner Production*, vol. 167, p. 55-67, nov. 2017, doi: 10.1016/j.jclepro.2017.08.131.
[61] A. Laborel-Préneron, J. E. Aubert, C. Magniont, C. Tribout, et A. Bertron, « Plant aggregates and fibers in earth construction materials: A review », *Construction and Building Materials*, vol. 111, p. 719-734, mai 2016, doi: 10.1016/j.conbuildmat.2016.02.119.
[62] J. Lima et P. Faria, « Eco-Efficient Earthen Plasters: The Influence of the Addition of Natural Fibers », in *Natural Fibres: Advances in Science and Technology Towards Industrial Applications*, vol. 12, R. Fangueiro et S. Rana, Éd. Dordrecht: Springer Netherlands, 2016, p. 315-327. doi: 10.1007/978-94-017-7515-1_24.
[63] U. Röhlen et C. Ziegert, *Earth Building Practice: Planning - Design - Building*. Beuth Verlag, 2011.
[64] L. Randazzo, G. Montana, A. Hein, A. Castiglia, G. Rodonò, et D. I. Donato, « Moisture absorption, thermal conductivity and noise mitigation of clay based plasters: The influence of mineralogical and textural characteristics », *Applied Clay Science*, vol. 132-133, p. 498-507, nov. 2016, doi: 10.1016/j.clay.2016.07.021.
[65] K. S. W. Sing, « Reporting physisorption data for gas/solid systems with special reference to the determination of surface area and porosity (Recommendations 1984) », *Pure and Applied Chemistry*, vol. 57, n° 4, p. 603-619, janv. 1985, doi: 10.1351/pac198557040603.
[66] T. Ashour, H. Georg, et W. Wu, « An experimental investigation on equilibrium moisture content of earth plaster with natural reinforcement fibres for straw bale buildings », *Applied Thermal Engineering*, vol. 31, n° 2, p. 293-303, févr. 2011, doi: 10.1016/j.applthermaleng.2010.09.009.
[67] M. Maddison, T. Mauring, K. Kirsimäe, et Ü. Mander, « The humidity buffer capacity of clay–sand plaster filled with phytomass from treatment wetlands », *Building and Environment*, vol. 44, n° 9, p. 1864-1868, sept. 2009, doi: 10.1016/j.buildenv.2008.12.008.
[68] A. Laborel-Préneron, « Formulation and characterization of unfired clay bricks with plant aggregates », Université de Toulouse, Université Toulouse III-Paul Sabatier, 2017.
[69] L. Soudani *et al.*, « Assessment of the validity of some common assumptions in hygrothermal modeling of earth based materials », *Energy and Buildings*, vol. 116, p. 498-511, mars 2016, doi: 10.1016/j.enbuild.2016.01.025.
[70] F. McGregor, A. Heath, E. Fodde, et A. Shea, « Conditions affecting the moisture buffering measurement performed on compressed earth blocks », *Building and Environment*, vol. 75, p. 11-18, mai 2014, doi: 10.1016/j.buildenv.2014.01.009.
[71] M. Hall et D. Allinson, « Assessing the effects of soil grading on the moisture content-dependent thermal conductivity of stabilised rammed earth materials », *Applied Thermal Engineering*, vol. 29, n° 4, p. 740-747, mars 2009, doi: 10.1016/j.applthermaleng.2008.03.051.
[72] P. M. Touré, V. Sambou, M. Faye, A. Thiam, M. Adj, et D. Azilinon, « Mechanical and hygrothermal properties of compressed stabilized earth bricks (CSEB) », *Journal of Building Engineering*, vol. 13, p. 266-271, sept. 2017, doi: 10.1016/j.jobe.2017.08.012.
[73] D. Medjelekh *et al.*, « Characterization of the coupled hygrothermal behavior of unfired clay masonries: Numerical and experimental aspects », *Building and Environment*, vol. 110, p. 89-103, déc. 2016, doi: 10.1016/j.buildenv.2016.09.037.

[74] B. Jiang, T. Wu, W. Xia, et J. Liang, « Hygrothermal performance of rammed earth wall in Tibetan Autonomous Prefecture in Sichuan Province of China », *Building and Environment*, vol. 181, p. 107128, août 2020, doi: 10.1016/j.buildenv.2020.107128.
[75] D. Lelièvre, T. Colinart, et P. Glouannec, « Modeling the Moisture Buffering Behavior of a Coated Biobased Building Material by Including Hysteresis », *Energy Procedia*, vol. 78, p. 255-260, nov. 2015, doi: 10.1016/j.egypro.2015.11.631.